Estimation of fracture toughness KIC from Charpy impact test data in T-welded connections repaired by grinding and wet welding

Article *in* Engineering Fracture Mechanics · March 2016

DOI: 10.1016/j.engfracmech.2015.12.010

5 authors, including:

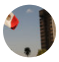

D. Angeles-Herrera
Instituto Mexicano del Petroleo

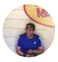

Julio César Velázquez
Instituto Politécnico Nacional

Martín Julián Fernández-Cueto
Tecnológico Nacional de México-Instituto Tecnológico de Tuxtepec

Engineering Fracture Mechanics 153 (2016) 351–359

Contents lists available at ScienceDirect

Engineering Fracture Mechanics

journal homepage: www.elsevier.com/locate/engfracmech

Estimation of fracture toughness K_{IC} from Charpy impact test data in T-welded connections repaired by grinding and wet welding

G. Terán [a,*], S. Capula-Colindres [b], D. Angeles-Herrera [c], J.C. Velázquez [a], M. J. Fernández-Cueto [d]

[a] Departamento de Ingeniería Química Industrial, ESIQIE, IPN, UPALM EDIF. 7, Zacatenco, México D.F. C.P. 07738, Mexico
[b] Instituto Politécnico Nacional, Centro de Investigación en Computación, Av. Juan de Dios Batiz s/n, Col. Nueva Industrial Vallejo, México D.F. 07738, Mexico
[c] Instituto Mexicano del Petróleo, Eje central Lázaro Cárdenas 152, Col. San Bartolo Atepehuacan, México D.F. C.P. 07730, Mexico
[d] Instituto Tecnológico de Tuxtepec, Av. Dr. Victor Bravo Ahuja s/n, col. 5 de Mayo, C.P. 68350 Tuxtepec, Oaxaca, Mexico

A R T I C L E   I N F O

Article history:
Received 4 June 2015
Received in revised form 7 December 2015
Accepted 12 December 2015
Available online 17 December 2015

Keywords:
Stress intensity factor
Charpy V-notch
Porosity
Grinding
Wet welding

A B S T R A C T

This work presents, for the first time, and estimation of fracture toughness K_{IC} correlations from Charpy V-notch (CVN) impact test data extracted from T-welded connections repaired with rectangular grinding and filled by wet welding. To obtain K_{IC} values, equations based on the yield stress (σ_{YS}) of the wet welding beads were used. The estimated K_{IC} data decreased with increasing water depth. These two characteristics (porosity and microstructures for low carbon steels) did not improve the mechanical properties, such as Charpy impact and K_{IC} values.

1. Introduction

Thus far, studies have demonstrated how to obtain the mechanical behavior of wet welding using different electrodes, water depths and metal bases [1–10]. The typical mechanical properties of characterization include the following: (i) yield stress (σ_{YS}); (ii) ultimate tensile stress (σ_{UTS}); (iii) Hardness Brinell (HB); (iv) Charpy V-notch (CVN) impact values; (v) porosity values; and (vi) the microstructures in the wet weld beads. However, a mechanical property that has not been reported in the specialized literature is the fracture toughness K_{IC}.

In linear elastic fracture mechanics (LEFM), K_{IC} is the magnitude of the stress intensity at the tip of the crack if the strain in the body is elastic [11]. At present, the ASTM E-399 standard [12] is used to obtain K_{IC} values in planar strain for the displacement mode of crack opening. This standard is complex and very costly. This is because it involves machining test specimens with complicated geometries under very strict tolerances. In addition, it is not always possible to prepare the specimens if the analyzed material does not have proper dimensions [13]. Nevertheless, it is possible to obtain K_{IC} values from the correlations of Charpy impact test values [14–26]. These correlations are based on CVN specimens. The impact energy values are used to determine the brittle-ductile transition temperature (BDTT) of the materials tested.

* Corresponding author.
E-mail addresses: gerardoteranm@gmail.com (G. Terán), selenecapula@gmail.com (S. Capula-Colindres), daherrera@imp.mx (D. Angeles-Herrera), jcva8008@yahoo.com (J.C. Velázquez), martinjfc@yahoo.com.mx (M. J. Fernández-Cueto).

http://dx.doi.org/10.1016/j.engfracmech.2015.12.010
0013-7944/

Nomenclature

CVN	Charpy V-notch
FA	acicular ferrite
FSA	ferrite aligned
FS	sideplate ferrite
FPG	grain border primary
E	Young's modulus
K_{IC}	fracture toughness
SMAW	shielded metal arc welding
σ_{YS}	yield stress

The K_{IC} value is a material property that is independent of the geometry of the planar strain. Thus, K_{IC} values can apply to a structure or element constructed from the same material [27]. Using correlations from a Charpy impact test, it is possible to obtain the K_{IC} values. Once the K_{IC} values are determined, it is necessary to understand the cracking behavior present in T-welded connections repaired by grinding and wet welding. It is well-known that fracture mechanics have two main objectives: to determine the mechanical strength of a cracked body and the crack propagation velocity [11].

In the present work, K_{IC} values were estimated from K_{IC}–CVN correlations reported in studies for CVN impact test data. CVN values were obtained from the work reported by Terán [9,10]. Charpy test specimens with standard dimensions (10×10 mm) and a V-notch of 60° were extracted at the weld toe from T-welded connections with rectangular grinding. Then, this grinding was filled by wet welding simulating water depths.

2. Experimental procedure

2.1. Wet welding

To employ wet welding techniques, the same procedure reported by Teran et al. [9,10] was used. T-welded connections were manufactured using ASTM A36 steel. Table 1 shows the chemical composition of the A36 steel, that is, the percent elements in mass. Rectangular grinding was at the weld toe in the T-welded connections. The width of the rectangular grinding was 4 mm, and two grinding depths of 6 mm and 10 mm were used at the weld toe. To create the rectangular grinding, conventional grinding equipment in air conditions was used. Shielded metal arc welding (SMAW) and E6013 coated electrodes were used to fill the rectangular grinding by the wet welding process. Vinilic resin was used to coat the electrodes. A hyperbaric chamber and gravity welding system (GWS) were used to simulate the water depths. The water depths were 50 m, 70 m and 100 m. Table 2 shows the variables used for the wet welding process.

Once the rectangular grinding was filled by wet welding, CVN energy data were obtained. Fig. 1a–c shows the Charpy specimen dimensions using the ASTM E23 [28], T-welded connections dimensions, and a T-welded connection filled by wet welding, respectively. The Charpy test temperature was 25 °C, and a Charpy machine model 74 with a capacity of 0.0–274 ft-lb was used following the recommendation of ASTM E23.

2.2. K_{IC}–CVN correlations

By determining the CVN impact energy values, the K_{IC} values using K_{IC}–CVN correlations could be estimated [14–26,29]. It was necessary to choose the behavior of the Charpy impact values, which depended on the interest zone, such as the brittle regime, transition regime, ductile regime, and σ_{YS} of the material and energy values. One of the main factors in obtaining Charpy impact energy values is the zone of ductile–brittle behavior for different temperatures. Fig. 2 shows the DBTT of A36 steel. To estimate fracture toughness, the following points are determined [30].

(1) A lower bound correlation for the brittle (lower shelf) regime. The equations can obtain the fracture toughness in the bottom, which is based on the T_{ref} temperature reference. The T_{ref} is used to calculate 20 J for carbon low steels and 27 J for steel alloys.

Table 1
Chemical composition of ASTM A36 steel [9].

Element (%)										
C	Si	Mn	P	S	Ni	V	Cu	Nb	Al	Ti
0.14	0.22	0.76	0.014	0.009	0.01	0.003	0.008	0.002	0.03	0.008

Table 2
Variables used for wet welding [9].

Applied current (A)	Electrode working angle (°)	Electrode diameter (mm)	Water depth (m)
160	60	2.4 and 3.2	50 and 70
190	55	2.4 and 3.2	100

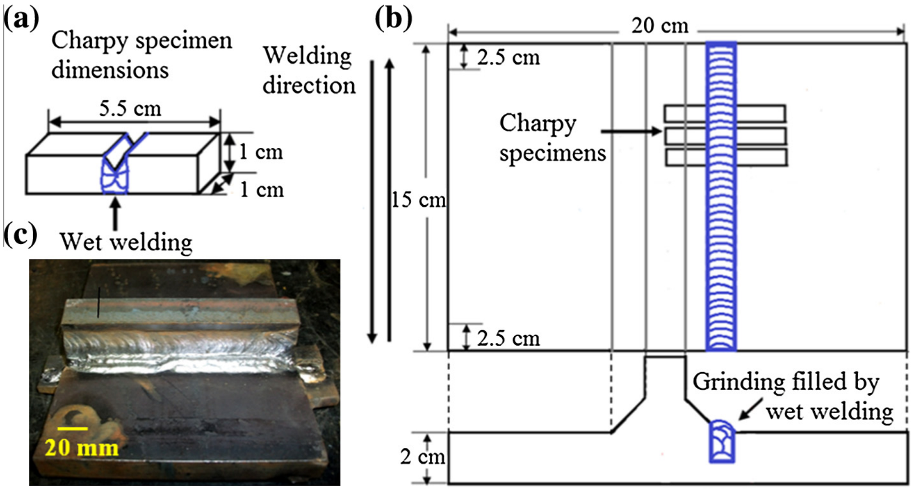

Fig. 1. T-welded connection, (a) Charpy specimen dimensions, (b) dimensions and (c) wet welding.

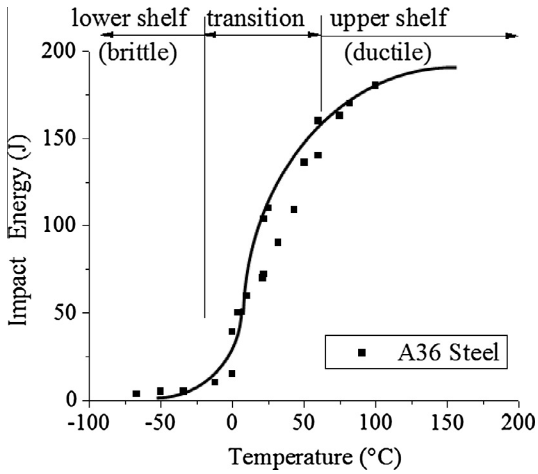

Fig. 2. CVN impact energy vs temperature, showing the DBTT for the A36 steel.

(2) A statistical method for the transition regime (the master curve). It is based on an established reference transition temperature.
(3) A lower bound correlation for the ductile (upper shelf) regime. If there is a temperature curve, data can be adjusted to a tangent to determine the relationship between the impact energy and temperature.

Table A1 shows the equations used to convert K_{IC}–CVN correlations from Charpy values for each zone in the energy–temperature curve. Although these Charpy values do not represent the real fracture toughness data, these values can be used as reference values to conduct mechanics fracture analysis.

A limitation in using CVN data to estimate fracture toughness is that Charpy data from the base metal may not be applicable when the material tested is welded or is located in the heat-affected zone (HAZ). Another limitation is that these data should come from a material with a representative microstructure and a proper temperature. However, there are no equations in the literature for weld beads and microstructures of wet weld beads. Based on these limitations, Table A1 in Appendix A. shows the traditional equations used for the wet weld beads.

Using the equations based on the σ_{YS} for the wet weld beads, the K_{IC} values could be estimated. The σ_{YS} of weld beads for different water depths and grinding depths were between 285 and 430 MPa [9,10]. In addition, Charpy impact tests were conducted at 20 °C and correspond to the transition zone in Fig. 3. These equations correspond to Barsom and Rolfe [18], Marandet and Sanz [24], Sailors and Corten [20] and Barsom and Rolfe [16]. The σ_{YS} used for the equations mentioned above were 275–1723 MPa, 268–923 MPa, and 303–820 MPa for Barsom and Rolfe [18], Marandet and Sanz [24] and Sailors and Corten [20], respectively. In Barsom and Rolfe [16], this equation could be applied in all zones of the energy–temperature curve. In addition, this equation used the σ_{YS} of the material.

3. Results and discussion

3.1. Charpy energy values

Table 3 shows the CVN test results [9] from previous works, and Table 4 presents the K_{IC} values evaluated according to different authors. This table also presents the σ_{YS} of the wet weld beads for each working condition. Fig. 3a presents CVN data against water depths, and Fig. 3b shows the comparison with other authors. Although these authors [1–8] used a temperature of 0 °C, the values were similar to the results obtained in the present work. This behavior is attributed to the porosity increasing with water depth. Teran et al. [9] reported porosity values of 3%, 5% and 10% for water depths of 50 m, 70 m and 100 m, respectively, for a 10-mm grinding depth. Additionally, for a 6-mm grinding depth, the porosity values were 2%, 4% and 8% for water depths of 50 m, 70 m and 100 m, respectively [9]. The porosity contributed to increasing the crack growths rates [32], which provided a favorable path for separating the fracture plane, resulting in low fracture toughness values [33]. Another important factor is that the microstructures presented for low carbon steels were ferrite aligned (FSA), ferrite sideplate (FS) and grain border primary (FPG) for different water depths [34]. It is well-known that to have high impact energy values, it is necessary to obtain acicular ferrite (FA). FA has a fine structure type "basket". Due to the orientation of this type, the grain can eliminate the crack propagation in the FA matrix. As mentioned above, the FA is the microstructural constituent that provides greater resistance for the material [35]. Then, for Charpy impact energy values in the present work, it could be said that these data are accepted and comparable with other authors who conducted Charpy impact tests at different temperatures. In addition, previous studies added metals in the coat of the electrodes to improve the performance in water conditions.

Most of the CVN specimens presented brittle behavior with low ductility, although the test temperature was 20 °C (see Fig. 4). In addition, the slag was trapped in the lower zone in each wet weld bead because the slag has a low density and the wet welding technique is too fast, so the slag becomes trapped in the wet weld beads. In addition, the grinding width (4 mm) did not help gases escape. In this case, the high porosity percentage and slag induced low CVN values. Moreover, the microstructures presented were not the best in terms of the ductile behavior in the CVN specimens.

3.2. K_{IC} values

For the case of the K_{IC} of A36 steel in air conditions, Ripling and Crosley [36] found that the K_{IC} value is 100 MPa $\sqrt{\text{m}}$ at 20 °C with a crack arrest toughness of 50.8 mm (2 in.) for A36 steel. For 25.4 mm (1 in.) crack arrest toughness, the K_{IC} value is 120 MPa $\sqrt{\text{m}}$. Murty et al. [37] found that the K_{IC} value of 130 MPa $\sqrt{\text{m}}$ for A36 steel at 25 °C represents the elastic–plastic fracture toughness parameter. Sovak [38] found K_{IC} values of 75.76–85.42 MPa $\sqrt{\text{m}}$ for the welding on A36 steel at −34 °C with a value of 13.6 J for full-thickness ASTM E399 specimens (4 in.). The fracture mode is governed by the fracture temper-

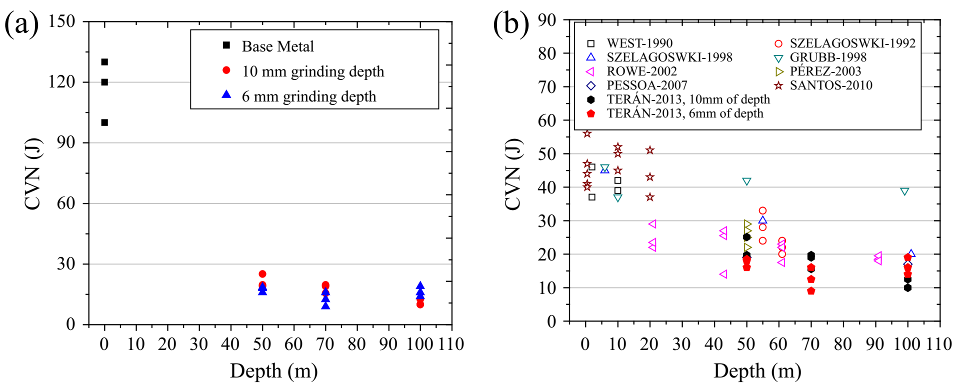

Fig. 3. CVN energy absorbed (a) in this work and (b) in previous studies [1–8].

Table 3
Mechanical property values for the different working conditions.

Welding depth (m)	Grinding depth (mm)	σ_{YS} (MPa)	Charpy at 20 °C (J)
50	10	430	19.0
50	10	372	19.7
50	10	409	25.1
70	10	363	19.0
70	10	365	19.7
70	10	318	15.6
100	10	301	10.0
100	10	323	12.5
100	10	285	10.0
50	6	410	16.0
50	6	392	18.0
50	6	382	18.5
70	6	376	16.0
70	6	327	12.5
70	6	364	9.0
100	6	347	19.0
100	6	316	16.0
100	6	357	14.0

Table 4
K_{IC} values for different authors.

Barsom and Rolfe [18] (MPa $\sqrt{m}$)	Marandet and Sanz [24] (MPa $\sqrt{m}$)	Sailor and Corten [20] (MPa $\sqrt{m}$)	Barsom and Rolfe [16] (MPa $\sqrt{m}$)
61.5	82.8	63.6	64.0
63.2	84.3	64.8	62.0
75.8	95.2	73.1	74.5
61.5	82.8	63.6	60.1
63.2	84.3	64.8	61.5
53.1	75.0	57.7	50.5
38.0	60.1	46.2	36.9
44.9	67.2	51.6	44.0
38.0	60.1	46.2	36.3
38.0	60.1	46.2	39.7
59.1	80.6	61.9	59.7
60.3	81.7	62.8	60.4
54.1	76.0	58.4	54.6
44.9	67.2	51.6	44.2
35.1	57.0	43.8	35.6
61.5	82.8	63.6	59.0
54.1	76.0	58.4	51.2
48.9	71.1	54.6	49.1

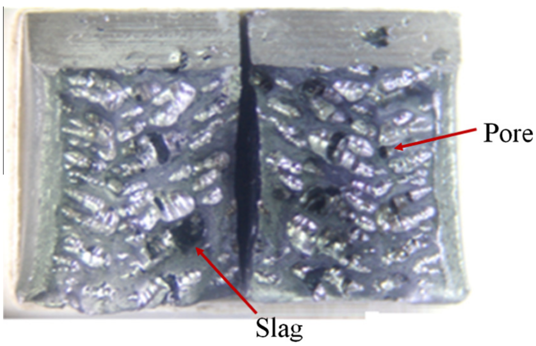

Fig. 4. Porosity on the fracture surface of the Charpy specimen for a 6 mm grinding depth and 50 m water depth [9].

ature, the rate at which loads are applied and the constraints that prevent plastic deformation. The effects of these limits on the fracture mode are reflected in the fracture toughness behavior of the material. Fracture toughness increases with increments of temperature, decreasing the load rate and constraints. There is no single fracture toughness value for steel, even at a fixed temperature and loading rate [36,38,39]. Thus, at a given temperature, the fracture toughness values measured at high loading rates are lower than those measured at lower loading rates; therefore, K_{IC} values can vary for the same material (laboratory conditions).

Table 3 shows the K_{IC} values for different working conditions. Fig. 5a and b shows the K_{IC} values obtained for different grinding depths of 10 mm and 6 mm, respectively. Additionally, the fracture toughness values for wet weld beads decreases with increasing water and grinding depth. This behavior occurs because the CVN values are proportional to K_{IC}, and the CVN data decrease due to the porosity percentage, microstructures and slag located in the wet weld beads. Generally speaking, Table 3 and Fig. 5a and b show that the K_{IC} values using the Marandet's equation [24] are higher than those using the four equations employed, for example, Sailors and Corten [20] and Barsom and Rolfe [16], which are similar, and finally Barsom and Rolfe [18]. For the sake of illustration, Fig. 6 is a box plot for different empirical models. In this graph, it is possible to observe that the values for Mandaret's model are always greater, whereas Sailor's model presents the result with the least uncertainty. Finally, the two Barsom models show quite similar results. This is because Marandet and Sanz [24] only used a constant of 19 to obtain K_{IC} values, whereas Sailors and Corten [20] used the Young's modulus (E) and a constant of 8. Barsom and Rolfe [16] employed the σ_{YS} at 0.2% in this equation to estimate the K_{IC} values. Finally, Barsom and Rolfe [18] also employed E and a constant of 2. The K_{IC} values in Table 3 are correlations obtained in an empirical way, which are valid in restricted ranges of data. Although the CVN impact test data do not represent true fracture toughness data, these data can be used as a starting point for determining the toughness in an assessment.

Although the equations in the transition zone of Fig. 2 were employed, these equations present a conservative grade [16,40]. It is necessary to propose more proper correlations to estimate the fracture toughness of K_{IC}–CVN correlations [41] for different steels, welding and microstructures that have a wide range of yield stress applied in different zones of the energy–temperature curve; this is because the K_{IC} values are conservative when they are applied to steels with low resistance (250 MPa) [18] and there are not K_{IC}–CVN correlations for wet weld beads or steels with different microstructures.

Yield strength, impact energy and shelf temperature are some of the issues used to validate relations in the specified range [27]. It is assumed that although in many cases the real values of fracture toughness cannot be estimated by calculating methods, these relations can be effective and useful in signifying and investigating the manner of the fracture toughness variations regarding the impact energy. In addition to the yield strength, the impact energy and shelf temperature are the parameters used to estimate the fracture toughness from the impact energy, and it is important to specify the role of microstructure [42]. Salemi [42] found that these variables are needed to specify the importance of the microstructure and to determine its mechanical behavior.

In the best case, the K_{IC} values must be compared with the values of specimens, as indicated by the ASTM E399 [12]. One of the shortcomings of this standard is the inevitable planar strain in experimental specimens and the cost and the statistical scattering of the values obtained from the test [42]. For steels of medium and low resistance of σ_{YS}, where the behavior is elastic plastic, to obtain a valid K_{IC} for a test implies the manufacturing of a specimen with large dimensions in the planar strain state. This would imply the use of a test machine that is sufficiently powerful to apply loads to this specimen [27].

The origin of the K_{IC}–CVN correlations are equations proposed from linear correlations between K_{IC}–CVN. Fig. 7a and b shows that the K_{IC}–CVN equations have a linear source. Fig. 7a shows a better behavior compared to Fig. 7b, with a greater distribution in K_{IC} values. These equations were made to correlate the Charpy impact energy with K_{IC} and to allow a quantitative assessment of critical flaw size and permissible stress levels. Therefore, these equations are valid only for limited types of material and ranges of data. However, these correlations provide a useful guide to estimate the fracture toughness. Thus, simple and empirical correlations can be used as general guidelines for estimating K_{IC} within the limits of the specific correlations. Although CVN impact test data do not represent true fracture toughness data, these data can be used as a starting point for determining the toughness to use in an assessment for T-welded connections repaired by grinding and wet welding.

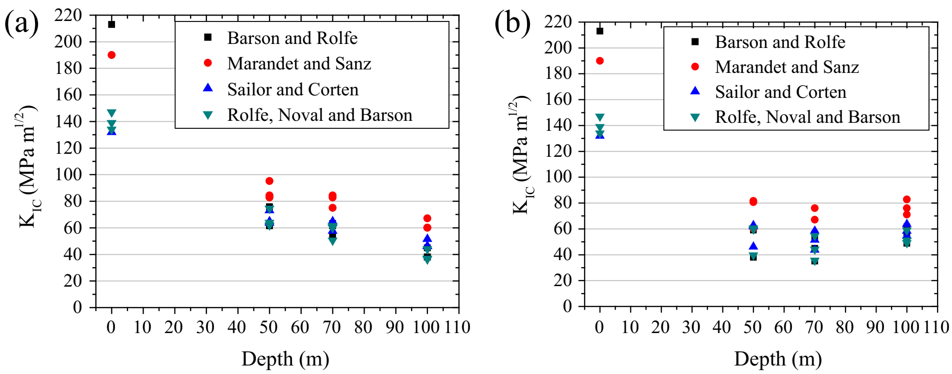

Fig. 5. K_{IC} value variations as a function of depth and grinding: (a) 10-mm grinding depth, and (b) 6-mm grinding depth.

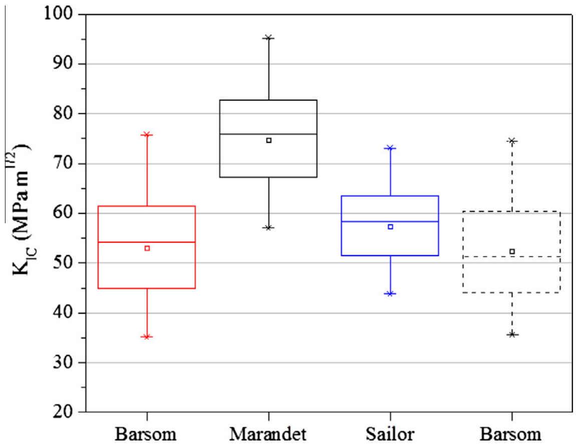

Fig. 6. Box plot for the K_{IC} values obtained for different empirical models.

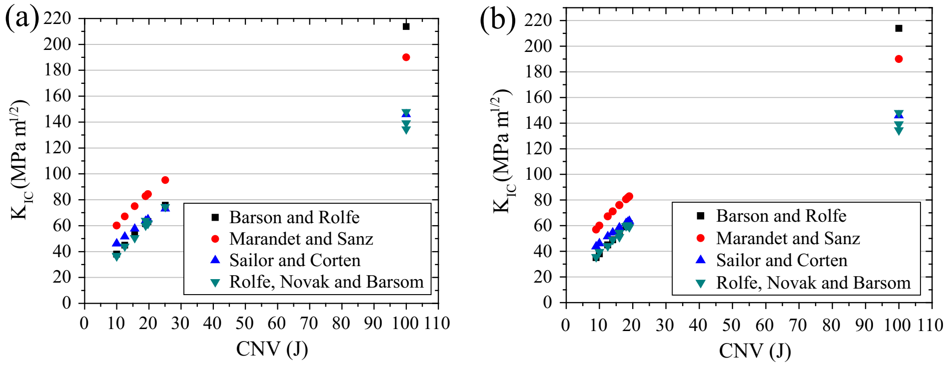

Fig. 7. K_{IC}–CVN correlation values: (a) 10-mm grinding depth and (b) 6-mm grinding depth.

4. Conclusions

Based on the results of this study, the following conclusions are made:

(1) The CVN energy values are comparable with those from previous studies, although in our case, the working temperature was 25 °C, whereas previous studies used temperatures below 0 °C. This is because at porosity percentages obtained, the slag found in wet welding beads and microstructures (FSA, FS, and FPG) presented in the wet welding.

(2) The K_{IC} value of A36 steel is 100–120 MPa $\sqrt{m}$ and varies by fracture, the rate at which loads are applied and the magnitude of the constraints that prevent plastic deformation. The effects of theses parameters on the fracture mode are reflected in the fracture toughness behavior of the material.

(3) The selection K_{IC}–CVN correlation equations is based on the base metal and materials with a representative microstructure and a proper temperature. Those equations cannot be applied to weld beads or material with defects, such as pores. Although, CVN impact test data do not represent true fracture toughness data, these K_{IC}–CVN correlation values can be used as a starting point for determining the toughness to be used in an assessment for T-welded connections repaired by grinding and wet welding. This is because K_{IC}–CVN correlations are based on the yield stress of the material.

(4) It was observed that the K_{IC} values decreased with increasing water depth; this is because these values are proportional to the CVN data. These K_{IC} values should be compared to the K_{IC} of cracking specimens according to the ASTM E399 standard. In addition, the porosity provided a favorable crack path to separate fracture planes, resulting in low fracture toughness.

(5) The K_{IC} data obtained from Marandet's equation are greater than those obtained from the four equations employed, that is, those of Sailor and Rolfe, which are similar, and Barsom. This is because Marandet only used a constant of 19 to obtain K_{IC} values, whereas Rolfe employed E and a constant of 8. Rolfe employed the yield stress at 0.2% in this equation. Finally, Barsom used E and a constant of 2 to obtain the K_{IC} values.

Appendix A

This appendix presents the K_{IC}-correlations for materials from the upper and lower shelf with different transition temperature, yield stress and Charpy energy values (see Table A1).

Table A1
K_{IC}–CVN correlations.

Upper shelf region		Range
Rolfe-Novak-Barson [16]		
$\left(\frac{K_{IC}}{\sigma_{ys}}\right)^2 = 0.64\left(\frac{CVN}{\sigma_{ys}} - 0.01\right)$	MPa $\sqrt{m}$, Mpa, J	760 < σ_{YS} < 170 MPa
$\left(\frac{K_{IC}}{\sigma_{ys}}\right)^2 = 5\left(\frac{CVN}{\sigma_{ys}} - 0.05\right)$	$ksi\sqrt{in}$, ksi, ft-lb	σ_{YS} > 689 MPa
		σ_{YS} > 100 ksi
WRC 265 [19]		
$\left(\frac{K_{IC}}{\sigma_{ys}}\right)^2 = 0.54\left(\frac{CVN}{\sigma_{ys}} - 0.02\right)$	MPa $\sqrt{m}$, Mpa, J	
$\left(\frac{K_{IC}}{\sigma_{ys}}\right)^2 = 4\left(\frac{CVN}{\sigma_{ys}} - 0.1\right)$	$ksi\sqrt{in}$, ksi, ft-lb	
Sailors and Corten [20]		
$\left(\frac{K_{IC}}{\sigma_{ys}}\right)^2 = 5\left(\frac{CVN}{\sigma_{ys}} - 0.0.5\right)$	$ksi\sqrt{in}$, ksi, ft-lb	1172–1344 MPa
		170–195 ksi, 100–110 ft-lb
Rolfe-Novak-Barson [17]		
$\left(\frac{K_{IC}}{\sigma_{ys}}\right)^2 = \frac{5}{\sigma_{ys}}\left(CVN - \frac{\sigma_{ys}}{20}\right)$	$ksi\sqrt{in}$, ksi, ft-lb	110–246 ksi, 16–89 ft.lb
Robert and Newton [22]		
$K_{IC} = 0.804\sigma_{ys}\left(\frac{CVN}{\sigma_{ys}} - 0.0098\right)^{0.5}$	MPa $\sqrt{m}$, Mpa, J	
Transition temperature region		
Barsom and Rolfe [18]		
$\frac{K_{IC}^2}{E} = 2\,(CVN)^{3/2}$	$ksi\sqrt{in}$, ksi, ft-lb	40–250 ksi, 4–82 J
WRC 265 [19]		
$K_{IC} = 9.35(CVN)^{0.63}$	$ksi\sqrt{in}$, ksi, ft-lb	
$K_{IC} = 8.47(CVN)^{0.63}$	MPa $\sqrt{m}$, J	
Sailors and Corten [20]		
$K_{IC} = 14.6(CVN)^{0.50}$	MPa $\sqrt{m}$, Mpa, J	410–480 MPa
		59–69 ksi
$K_{IC} = 15.5(CVN)^{0.50}$	$ksi\sqrt{in}$, ksi, ft-lb	5 ft.lb < cu < 50 ft.lb
Sailor–Corten [20]		
$\frac{K_{IC}^2}{E} = 8(CVN)$	$psi\sqrt{in}$, CVN = ft-lbf, E = psi	268–923 MPa
		39–134 ksi
		5 ft.lb < cu < 50 ft.lb
Wullaert–Server [21]		
$K_{IC} = 2.1(\sigma_{ys}CVN)^{1/2}$	$ksi\sqrt{in}$, ksi, ft-lb	
Marandet and Sanz [24]		
$K_{IC} = 19(CVN)^{1/2}$	MPa $\sqrt{m}$, Mpa, J	303–820 MPa
		43–118 ksi
Lower shelf region		
Robert and Newton [22]		
$K_{IC} = 8.47(CVN)^{0.63}$	MPa $\sqrt{m}$, J	
INSTA [31]		
$K_{IC} = 12\sqrt{CVN}$	MPa $\sqrt{m}$, J	
Different zones		
Barsom and Rolfe [16]		
$K_{IC} = R_{p0.2}\sqrt{\frac{5}{R_{p0.2}}\left(CVN - \frac{R_{p0.2}}{20}\right)}$	$ksi\sqrt{in}$, ksi, ft-lb	

Acknowledgements

The authors thank the ESIQIE-IPN, CONACYT México and the Mexican Institute of Petroleum for the financial and material support.

References

[1] Szelagowski P, Pachniuk I, Stuhff H. Wet welding for platform repair. Int Soc Offshore Polar Engng 1992:208–15.
[2] Santos VR, Monteiro MJ, Assuncao FRC, Bracarense AQ, Pessoa EC, Marinho RR, et al. Evaluation and development of electrodes for wet welding of structural ship steels. OMAE 2010;20808:1–9.
[3] West TC, Mitchell G, Lindberg E. Wet welding electrode evaluation for ship repair. Weld J 1990;69(8):46–56.
[4] Perez-Guerrero F, Liu S, Smith C, Rodriguez-Sanchez E. Effect of nickel on toughness of underwater wet welds. OMAE 2003;37261:1–6.
[5] Rowe MD, Liu S, Reynolds TJ. The effect of ferro-alloy additions and depth on the quality of underwater wet welds. Weld J 2002;81:156S–66S.
[6] Pessoa EC. Estudo da variação da porosidade ao longo do cordão em soldas subaquática molhadas, (PhD thesis). Federal University of Minas Gerais; 2007.
[7] Szelagowski P. Wet welding as a serious repair procedure? J Offshore Mech Arctic Engng 1998;120(3):191–6.
[8] Grubbs CE, Reynolds TJ. State of the art underwater wet welding. July ed. World Oil; 1998. p. 79–83.
[9] Teran G, Cuamatzi-Meléndez R, Albiter A, Maldonado C, Bracarense AQ. Characterization of the mechanical properties and structural integrity of T-welded connections repaired by grinding and wet welding. Mater Sci Engng A 2014;599:105–15.
[10] Teran G, Cuamatzi-Meléndez R, Albiter A. Combination of techniques of grinding and underwater welding for repair cracks in welded connections. Mater Sci Forum 2014;793:51–8.
[11] Velázquez JL. Mecánica de fractura. México: Limusa; 2004.
[12] ASTM E-399. Standard test method for linear-elastic plane-strain fracture toughness KIC of metallic materials; 2009.
[13] Matusevich AE, Mancini RA, Giudici AJ. Determinación de la tenacidad a la fractura del material de un gasoducto. Rev Lantin Am Metal Mater 2012;32 (2):253–60.
[14] McNicol RC. Correlations of Charpy test results for standard and nonstandard size specimens. WRC; 1965. p. 385.
[15] Phaal R, Macdonald KA, Brown PA. Correlations between fracture and Charpy impact energy, report from the cooperative research programmed for industrial members only, TWI report 504/1994. Cambridge, U.K.: The Welding Institute; 1994.
[16] Barsom JM, Rolfe ST. Fracture and fatigue control in structures. 3rd ed. Englewood Cliffs, New Jersey: Prentice Hall; 1999.
[17] Rolfe ST, Novak SR. Slow-bend KIC testing of medium high-toughness steel. Review of development in plane strain fracture toughness testing, ASTM STP 463, ASTM; 1970. p. 124–59.
[18] Barsom JM, Rolfe ST. Correlations between KIC and Charpy V-notch test results in the transition-temperature range. Impact Testing of Metals, ASTM STP 466, ASTM; 1970. p. 281–302.
[19] Roberts R, Newton C. Interpretive report on small scale test correlations with KIC data, WRC Bulletin, Welding Research Council, New York N.Y.; February 1981. p. 265.
[20] Sailors RH, Corten HT. Relations between material fracture toughness using fractures mechanics and transition temperature test. In: Fracture toughness, proceeding of the 1972, National Symposium on Fracture Mechanics – Part II, STP 514, ASTM; 1972. p. 164–91.
[21] Wullaert RA. Fracture toughness predictions from Charpy V-notch data, what does the Charpy test really tell us? In: Proceeding of the American Institute of Mining, Metallurgical and Petroleum Engineers, American Society for Metals; 1978.
[22] Roberts R, Newton C. Report on small-scale test correlations with K_{IC} data. Weld Res Council Bull 1984;299.
[23] Barsom JM. The development of AASHTO fracture toughness for bridge steel. Engng Fract Mech 1975;7(3):605–18.
[24] Marandet B, Sanz G. Evaluation of the toughness of the medium-strength by using elastic fracture mechanics and correlations between KIC and Charpy V-notch, Flaw Growth and Fracture, STP 631, ASTM; 1977. p. 72–95.
[25] Norris DM, Reaugh JE, Server WL. A fracture-toughness correlations based on Charpy initiation energy. In: Fracture Mechanics: Thirteenth Conference, STP 473, ASTM; 1981. p. 207–17.
[26] Walling K. New report methodology for selecting Charpy toughness criteria for thin high strength steels. Report Represented to Commission X, IIW 1994, Annual assembly, Beijing, IIW DOC. NO. X.1290-94; 1994.
[27] Morales FR, Scott AD, Nápoles NP. Determinación de la tenacidad a la fractura de muestras de acero 45 fundido, empleando las correlaciones entre el K_{IC} y la energía de impacto medida en el ensaye de Charpy. Ingeniería Mecánica 2005;2:29–33.
[28] ASTM E23-12. Standard test methods for notched bar impact testing of metallic materials; 2012.
[29] British Steel, structural integrity assessment procedures for european industry SINTAP, sub-task 3.3 report: final issue determination of fracture toughness from Charpy impact energy: procedure and validation; 1998.
[30] API RP 579/ASME FFS, Fitness for service; 2007.
[31] INSTA Technical Report. Assessment of structures containing discontinuities. Stockholm: Materials Standards Institution; 1991.
[32] Ayaso FJ, Gonzalez B, Toribio J. Influencia de las inclusiones sobre el comportamiento en fractura de aceros perlíticos trefilados. Anal Mecánica Fract 2007;1:99–104.
[33] Broek D. Elementary engineering fracture mechanics. 4th ed. The Netherlands: Martinus Nijhoff; 1986. p. 8–19.
[34] Metals Handbook, 7th, vol. 6, Welding, Brazing and Soldering, ASM International; 2005.
[35] Sanchez A, Liu S, Olson D. Soldadura submarina mojada, 2do Congreso internacional de la soldadura en México, Monterrey, México; 1994. p. 179–89.
[36] Ripling EJ, Crosley PB. Crack arrest fracture toughness of a structural steel A36. Weld Res Suppl 1982:65s–74s.
[37] Murty KL, Mathew MD, Wang Y, Shan VN, Haggag FM. Nondestructive determination of tensile properties and fracture toughness of cold worked A36 steel. Int J Pres Ves Pip 1998;75:831–40.
[38] Sovak JF. The fracture resistance of 4-in thin A36 and A588 grade A electroslag weldments. Weld Res Suppl 1981:269s–72s.
[39] Federal Emergency Management Agency FEMA-355A, State of the Art Report on Base Metals and Fracture; 2000. p. 3-12–3-17.
[40] Saba BM. Evaluation of mechanical fitness for service of high temperature hydrogen attacked steel, A Thesis for Master of Science in Mechanical Engineering, Louisiana State University; 1994.
[41] Kapp JA, Underwood JH. Correlation between fracture toughness, Charpy V-notch impact energy and yield strength for ASTM A723 steel, Memorandum Report ARCCB-MR-92008; 1992.
[42] Salemi A. The effect of microstructure on estimation of the fracture toughness (K_{IC}) rotor steel using Charpy absorbed energy (CVN). J Adv Mater Process 2013;1(3):11–7.